Transactions of the Korean Nuclear Society Spring Meeting
Jeju, Korea, May 7-8, 2015

Severe Accident Progression and Consequence Assessment Methodology Upgrades in ISAAC for Wolsong CANDU6

Y.M. Song [a*], D.H. Kim [a], Sunil Nijhawan [b]
[a]*Korea Atomic Energy Research Institute, Severe Accident and PHWR Safety Research Division, P.O.Box 105, Yusong, Taejon, Korea, 305-600*
[b]*Prolet Inc., 98 Burbank Drive, Toronto, Ontario, CANADA, M2K 1N4*
[*]*Corresponding author: ymsong@kaeri.re.kr*

1. Introduction

There have been quite significant advances in understanding of CANDU core degraded behavior since ISAAC [1] was developed from a MAAP PWR code [2] for application to Wolsong CANDU reactors over 20 years ago. The code consists of a large number of models that are common with those for PWRs and some models that had been specifically developed for adaptation of MAAP to CANDUs. The code has served well its original intent and provided useful information about CANDU severe accidents [3]. However, present requirements that evolved since Fukushima as well as internal reviews recommend a need for upgrades to the CANDU specific features of the code. Simultaneous development of a new state of the art CANDU specific severe accident analysis code ROSHNI provides an opportunity to implement a number of its features within ISAAC.

Amongst the applications of integrated severe accident analysis codes like ISAAC, the principal are to a) help develop an understanding of the severe accident progression and its consequences; b) support the design of mitigation measures by providing for them the state of the reactor following an accident; and c) to provide a training platform for accident management actions. After Fukushima accident there is an increased awareness of the need to implement effective and appropriate mitigation measures and empower the operators with training and understanding about severe accident progression and control opportunities. An updated code with reduced uncertainties can better serve these needs of the utility making decisions about mitigation measures and corrective actions. Optimal deployment of systems such as PARS and filtered containment venting require information on reactor transients for a number of critical parameters. Thus there is a greater consensus now for a demonstrated ability to perform accident progression and consequence assessment analyses with reduced uncertainties. Analyses must now provide source term transients that represent the best in available understanding and so meaningfully support mitigation measures [4]. This requires removal of known simplifications and inclusion of all quantifiable and risk significant phenomena.

Advances in understanding of CANDU6 severe accident progression reflected in the severe accident integrated code ROSHNI are being incorporated into ISAAC using CANDU specific component and system models developed and verified for Wolsong CANDU 6 reactors. A significant and comprehensive upgrade of core behavior models is being implemented in ISAAC to properly reflect the large variability amongst fuel channels in feeder geometry, fuel thermal powers and burnup. The aim is to not only apply a best effort methodology but also to do so without any unnecessary simplifications providing sufficient detail so that transients in source terms (combustible gas, fission products) are captured in a detail consistent with response characteristics of the mitigation equipment. The upgrades result in a ~10 fold increase in core nodalization, evaluation of flows through the channels and inclusion of phenomena such as gradual boiloff of liquid inventory within the fuel channel, heatup and oxidation of end fittings and feeders. Preliminary results show that these have a profound effect on source terms as well as timing of events. There also are significant improvements in modeling of core debris and inclusion of additional failure models for fuel bundles, channels, vessels and structures. The code improvements provide stronger bases for increased confidence in results and allow the users to perform sensitivity analyses with enhanced confidence. The paper summarizes the models that have been added and provides some results to illustrate code capabilities.

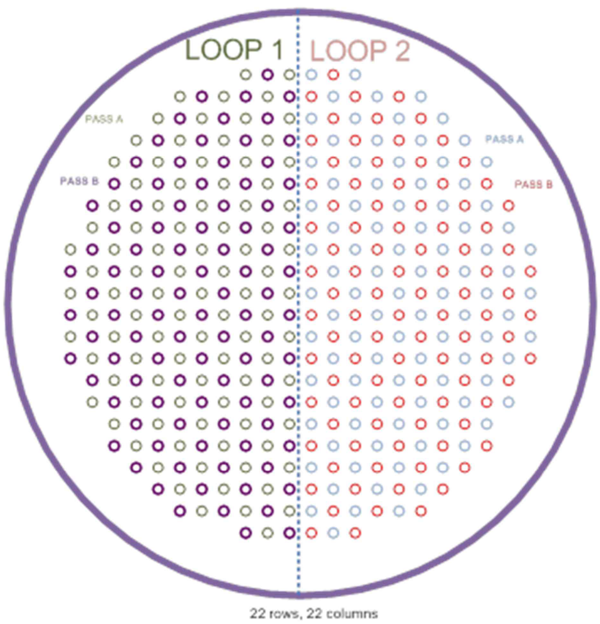

Fig. 1. New ISAAC modeling of all fuel channels

2. Upgrades to Core modeling

Geometrically, all fuel bundles in all 380 Wolsong fuel channels are exactly the same. Channels belong to one of the 2 flow loops (each half of the core) and to one of the 2 flow passes within each loop (adjacent channels are in opposite passes) – Fig. 1. However channels differ from each other in total thermal power, axial power profile (Fig. 2), burnup and feeder geometry.

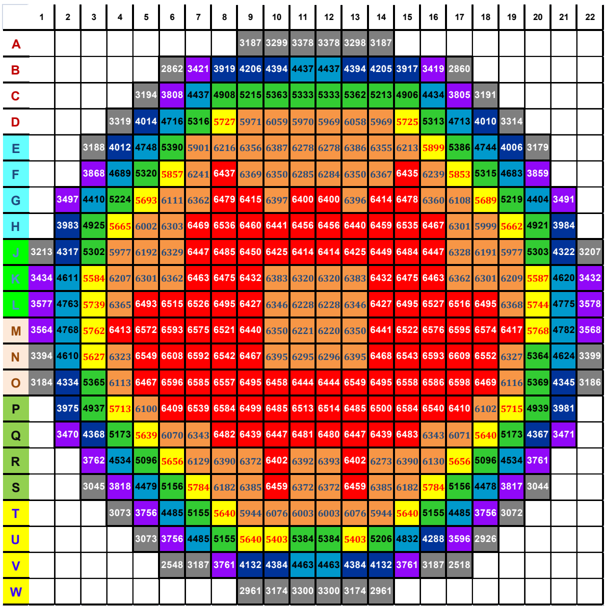

Fig. 2. Channel power map for Wolsong - 8 groups of channel power (See map below with channel power groups in kW)

Power Groupings	
7500	6400
6400	5900
5900	5400
5400	4900
4900	4400
4400	3900
3900	3400
3400	1

Vertical location of a channel within the core also determines its response to a loss of cooling event by the boundary conditions imposed on the channel by the moderator. Just the free volume inside feeders has an appreciable effect on the time at which a particular channel would heatup and degrades under steam flow conditions. The feeder design criterion is based on trying to flow-power match the feeders so that their exit fluid enthalpy is roughly the same for all the channels.

Thus it was decided to model all fuel channels and reduce any errors that may be caused by an averaging process. Recognizing that the individual channel response to a degradation in cooling is a strong function of location of the channel within the core, the thermal hydraulic and thermo-mechanical-chemical response of all fuel channels and all fuel bundles is modeled with considerations of variations in power, axial power profiles, fuel burnup, feeder geometries and external boundary conditions including presence of debris, proximity to in-core devices and other thermal hydraulic boundary conditions. This entails modeling of each of the 12 bundles in each of the 380 channels along with their 760 feeders and 760 end fittings. This level of detail facilitates a more detailed evaluation of source terms for energy, fission product and combustible gas loads to the containment and development of more realistic accident management strategies. The earlier ISAAC model treated 18 fuel channels per loop.

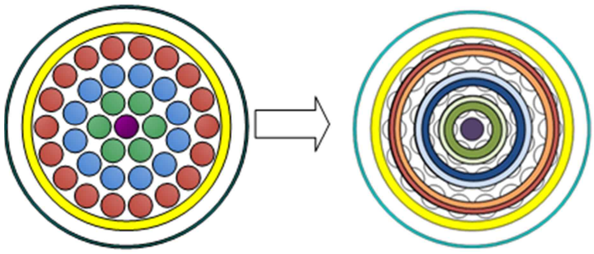

Fig. 3. Bundle model for degraded steam flow conditions

The fuel bundle modeling is significantly revamped. Previous model represented a fuel bundle as a single pin radiating to the pressure tube. The new model represents a fuel bundle with 14 concentric rings with two additional rings for pressure and calandria tube and considers flow within the 4 flow subchannels (Fig. 3). With 16x12x380 thermal nodes, the core thermal behavior is captured in unprecedented detail.

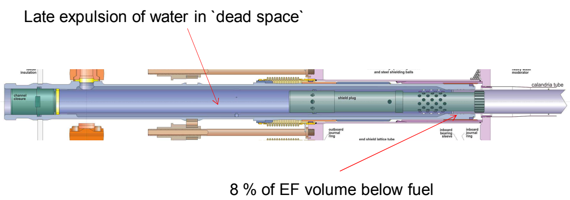

Fig. 4. End Fitting

End fittings and feeders were not modeled in ISAAC previously. Each end fitting is about 240 kg and presents a heat transfer path for the PHTS fluid into the end shields. They may also retain fluid within them (Fig. 4) while the channels are completely voided. Their direct exposure to hot steam exiting the channels prompts an investigation into their oxidation potential.

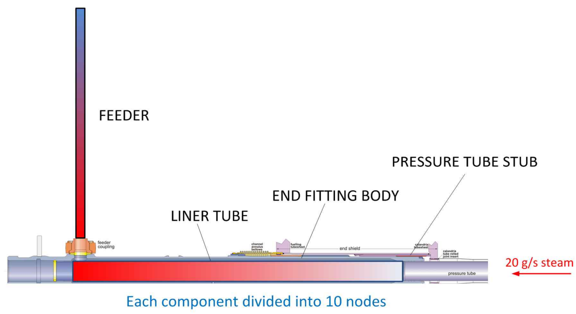

Fig. 5. End fitting and feeder heatup model

A model has been developed to calculate thermo-chemical response of end fittings and feeders. The model also includes the ~6.5 cm extension of pressure tube within the end fitting and treats the end fitting body, liner tube with 10 axial nodes. Feeders, which are located inside an insulated feeder cabinet, are also represented by 10 axial nodes (Fig. 5).

Feeders are about 9.2 km in length in total and about 1800 m^2 in surface area available for heat transfer and oxidation. Scoping analyses confirmed that both feeders and end fittings have a significant effect on a severe accident transient – both as heat sinks and as sources of deuterium gas. In the updated ISAAC, they are modeled in a number of different models depending upon the accident progression stage. The most significant effect of feeders is in their oxidation by hot steam exiting degraded fuel channels. Thus thermal response of all 760 end fittings and potential oxidation of 760 carbon steel feeders are now computed and a better accounting of heat sources and heat sinks is now implemented.

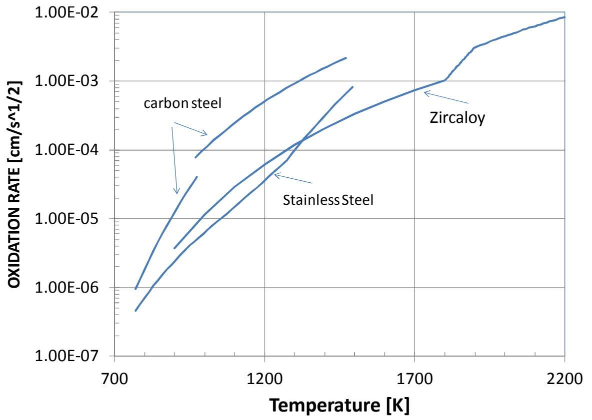

Fig. 6. Kinetics of oxidation of carbon steel feeders, stainless steel end fittings and zircaloy sheaths

Fig. 6 shows the oxidation rate expressed as increase in oxide thickness for the structural materials of interest – stainless steel in end fittings, carbon steel in feeders and zircaloy in the fuel channel. It is interesting to note that the carbon steel oxidation, exothermic in nature similar to zircaloy, is faster than for zircaloy [5]. It is also noted that while growth of a stable oxide on a zircaloy surface would tend to slow down oxidation, the Wustite (FeO) oxide is unstable and subject to peeling off. Modeling of steel oxidation can now also be extended to other steel surfaces such as the headers and main PHTS pipes.

3. Bundle and Channel Models

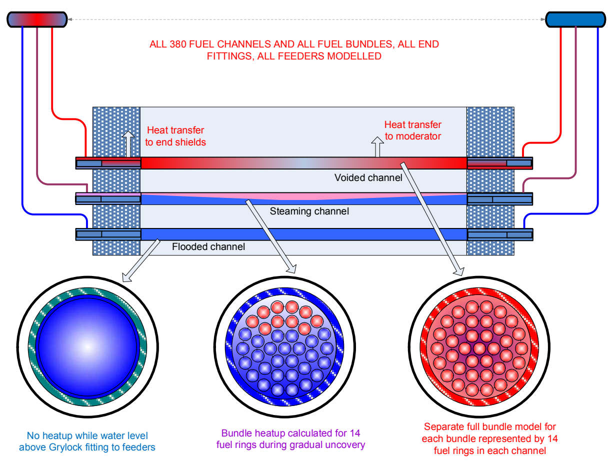

Fig. 7. Fuel channel heatup models

Reactor core and channel thermal hydraulic response is modeled in three stages (Fig. 7).

1. High PHTS fluid inventory, flooded channels
2. Depleting PHTS fluid Inventory, fuel bundles partially covered
3. Low PHTS fluid inventory, fuel bundles heating up in steam environment

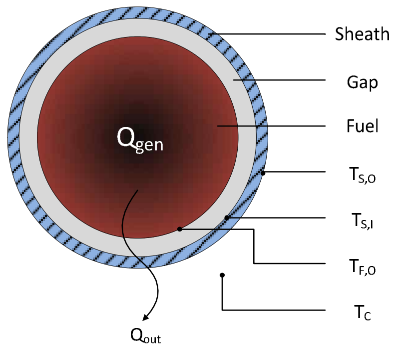

Fig. 8. Fuel modeling under conditions of adequate cooling

The first period of high fluid inventory is after a reactor trip and prior to uncover of any part of any fuel bundle in any channel. During this period, the decay heat from fuel channels is removed either by thermo-syphoning or bulk boiloff. Fuel temperatures are evaluated using a simple internal heat generation model for a fuel pin (Fig. 8).

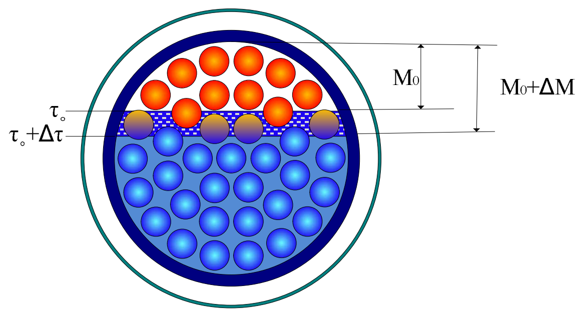

Fig. 9. Model for fuel heatup under channel boiloff conditions

During the period of liquid boiloff, a new model for fuel heatup by gradual partial uncovery is used (Fig. 9). While the water level in the channel is assumed to be the same in all bundle locations, local heat generation and removal rates consistent with local sub-channel flows and steam temperatures are used to evaluate transient fuel temperatures.

Fuel heatup upon gradual uncover is first calculated based on uncover of actual fuel rings and then assigned to the model of fuel and sheath rings associated with each actual fuel ring (central, inner, intermediate or outer). Calculations are performed sequentially for all fuel bundles in a channel and the water level is taken to be same in all fuel bundles in a given channel at a given time.

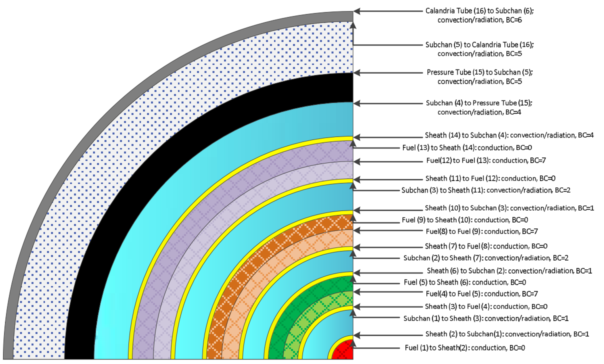

Fig. 10. Sixteen ring, dual surface bundle model

For evaluation of fuel heatup under steam flow conditions, the fuel geometry is represented by a generalized, multi-node annular ring model (Fig. 10). Each ring is modeled in such a way that it preserves the material properties, areas and volumes characteristic of the component it represents. The number of rings chosen is 16; the last two represent the pressure tube and the calandria tube. The three fuel element rings (containing 6, 12 and 18 fuel elements) are subdivided into two radial nodes each. The division is along the pitch circle diameters of the actual fuel element rings. Each actual fuel ring is modeled by two fuel rings with separate sheaths.

Flow through the fuel channels is calculated iteratively for both intact and disassembled channels. There are a number of options for channel flow calculations with the limitation of the user inferring header to header pressure drop from external analyses. User can also specify any of a number of distributions of channel flows. Momentum equation is solved for each channel between the headers.

4. Moderator models

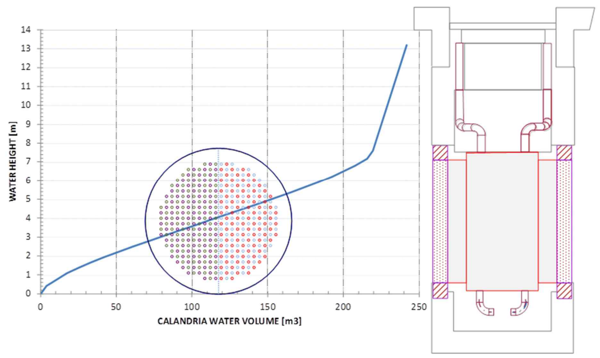

Fig. 11. Calandria vessel level including effect of channels and in-core devices

The calandria vessel is modeled with consideration for the location of in-core devices and a volume to level correlation developed within the code during input data post processing (Fig. 11). Heat transfer from the calandria vessel to the end shields and to the reactor vault is modeled with consideration of changes in fluid properties and fluid levels within the three volumes.

Voided space in the moderator upon depletion of water is modeled interactively with the channel and debris models. A 22x22x12 distribution of steam flow and temperatures is used for evaluation of heat exchange with intact fuel channels and debris.

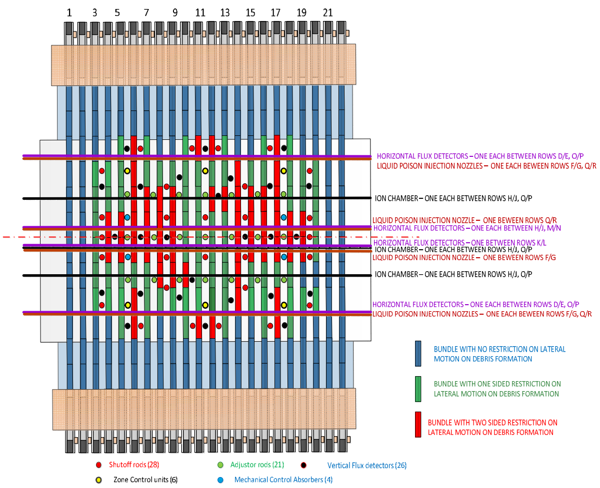

Fig. 12. Consideration of in-core devices

Effect of in-core devices (Fig. 12) is included during evaluation of debris movement and water level changes with water depletion in the moderator.

5. Failure Models

Models are included for the following:

1. Sheath failures
2. Bundle failure at high pressures
3. Bundle failures at low pressures
4. Pressure tube/calandria tube perforation due to strain
5. Calandria vessel failures due to thermal strain from debris.
6. Heat transport system failures due to over pressure
7. Reactor vault failures due to over pressure

6. Debris modeling

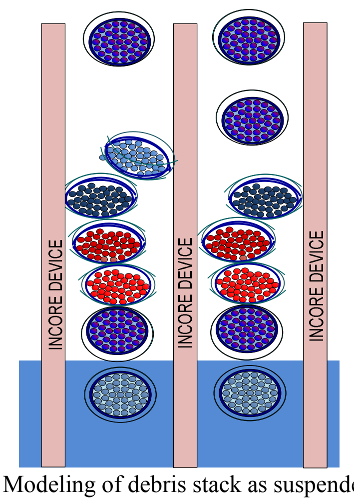

Fig. 13. Modeling of debris stack as suspended debris

Debris formed by disassembly of a fuel channel segment is tracked on a per fuel bundle basis (Fig. 13). When supported by underlying debris and constrained by in-core devices from dropping into the moderator, the debris are termed 'suspended debris'. Their interaction with steam environment for heat loss and oxidation is modeled for each dissociated fuel bundle (Fig. 14). Separate consideration is given to pressure tube/calandria tube segments and the fuel bundle compaction is modeled by specifying area available for heat transfer and oxidation.

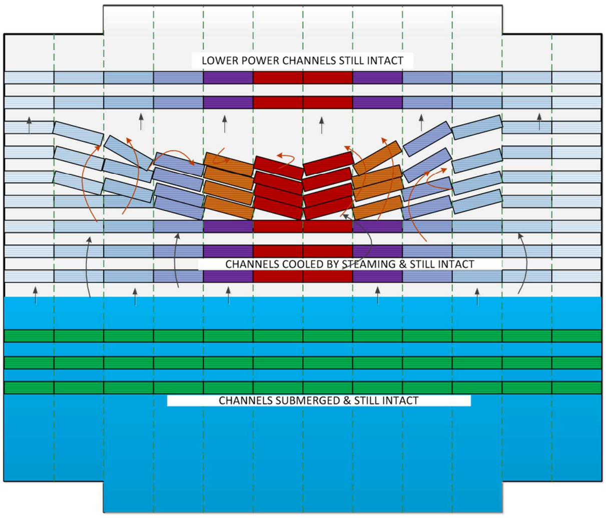

Fig. 14. Moderator gas space modeling for suspended debris interaction with steam

Debris interaction with underlying channels includes consideration of channel rolled joint pull out both of calandria tube and pressure tube.

7. Sample results for early part of a SBO scenario

	1	2	3	4	5	6	7	8	9	10	11	12	13	14	15	16	17	18	19	20	21	22
A									1006	962	924	924	962	1007								
B						1249	1014	1056	1142	1094	998	998	1094	1142	1057	1014	1250					
C					1055	969	1082	958	930	998	982	982	998	930	958	1082	970	1056				
D				1054	1005	1048	940	1016	972	964	990	990	964	972	1016	940	1048	1006	1056			
E			1322	1034	1054	962	946	992	1034	1045	1154	1154	1045	1034	993	947	964	1055	1036	1327		
F			1064	1146	1010	990	1016	1056	1036	1074	1098	1098	1074	1036	1056	1016	990	1010	1148	1067		
G		1202	1260	1012	1037	1054	1014	1049	1066	1065	1116	1116	1065	1066	1050	1014	1055	1038	1014	1262	1204	
H		1361	1113	1121	1114	1092	1057	1121	1110	1100	1151	1151	1100	1110	1122	1058	1092	1114	1121	1114	1360	
J	1292	1284	1167	1142	1335	1298	1292	1307	1300	1286	1208	1208	1286	1300	1307	1292	1298	1336	1142	1166	1280	1294
K	1246	1250	1172	1228	1406	1353	1340	1374	1344	1346	1240	1240	1346	1344	1374	1340	1353	1381	1228	1170	1246	1244
L	1412	1305	1351	1570	1637	1512	1656	1734	1804	1780	1141	1141	1780	1804	1734	1656	1510	1635	1568	1348	1298	1408
M	1478	1380	1398	1562	1632	1688	1688	1803	1903	1892	1302	1302	1891	1902	1802	1687	1686	1630	1560	1395	1372	1472
N	1594	1468	1494	1588	1718	1622	1698	1858	1912	1938	1341	1341	1938	1910	1857	1696	1620	1715	1584	1490	1459	1588
O	1858	1647	1754	1614	1692	1664	1709	1866	1938	2002	1368	1368	2002	1937	1864	1707	1662	1688	1610	1749	1638	1852
P		1787	1928	1622	1784	1800	1788	1864	1954	1998	2018	2018	1998	1952	1864	1787	1798	1782	1618	1924	1780	
Q		1852	1766	1814	1746	1936	1819	1948	2002	2143	2113	2113	2143	2002	1947	1818	1934	1744	1812	1764	1848	
R			1868	1930	1997	1804	1942	2026	2120	2170	2266	2266	2170	2119	2024	1940	1802	1996	1928	1864		
S			2287	2174	2114	1988	1844	2090	2202	2432	2456	2456	2432	2202	2089	1842	1986	2112	2173	2287		
T				2300	2043	2002	2028	1987	2346	2377	2514	2514	2376	2345	1986	2028	2000	2042	2298			
U					2492	2150	2245	2548	2257	2356	2404	2403	2355	2256	2546	2244	2150	2491				
V						3023	2625	2373	2562	2430	2438	2438	2430	2561	2372	2624	3021					
W									3139	2992	3138	3138	2992	3138								

Fig. 15. Time period over which various channels boiloff the water within their feeders

Front end results for a station blackout scenario (SBO) are summarized below. Fig. 15 shows the range of time at which the water in the feeders is boiled off and the channels begin to void. The time at which the water in the heat transport system has drained to the level of the headers is taken as time zero in this illustration. It is evident that a significant variability exists even in the time at which the first channel begins to just void.

	1	2	3	4	5	6	7	8	9	10	11	12	13	14	15	16	17	18	19	20	21
A									5464	5371	5300	5300	5372	5466							
B						5790	5318	5028	4918	4786	4642	4642	4788	4919	5030	5319	5792				
C					5488	5060	4750	4204	3958	3936	3940	3940	3936	3960	4206	4753	5062	5492			
D				5400	4960	4470	3918	3755	3586	3536	3608	3608	3536	3587	3756	3921	4474	4962	5406		
E			5605	4974	4449	3900	3604	3503	3492	3492	3654	3654	3492	3492	3504	3607	3904	4455	4979	5614	
F			5065	4593	3992	3672	3521	3478	3488	3538	3593	3593	3538	3490	3479	3523	3674	3996	4601	5072	
G		5351	4886	4052	3806	3620	3460	3451	3496	3505	3558	3558	3505	3498	3452	3462	3622	3810	4056	4890	5355
H		5154	4366	3904	3731	3574	3468	3511	3528	3526	3575	3575	3526	3528	3512	3470	3576	3734	3906	4368	5150
J	5579	4944	4161	3765	3880	3778	3722	3732	3742	3741	3666	3666	3741	3742	3732	3722	3780	3882	3764	4158	4936
K	5422	4767	3995	3746	3902	3816	3761	3805	3799	3826	3743	3743	3826	3799	3804	3760	3816	3830	3744	3990	4747
L	5416	4695	4098	4033	4053	3908	4062	4172	4282	4299	3678	3678	4298	4282	4170	4059	3905	4048	4028	4088	4670
M	5455	4769	4131	3998	4006	4053	4066	4226	4375	4409	3846	3846	4407	4372	4222	4062	4048	4000	3990	4120	4740
N	5607	4903	4302	4056	4096	3966	4060	4266	4364	4430	3844	3844	4428	4361	4262	4056	3960	4087	4048	4289	4888
O	5821	5127	4730	4176	4098	4012	4065	4256	4370	4460	3798	3798	4458	4368	4251	4060	4006	4090	4166	4717	5112
P		5370	5026	4387	4364	4244	4172	4236	4371	4428	4438	4438	4427	4368	4234	4168	4237	4358	4379	5020	5360
Q		5662	5174	4872	4568	4546	4292	4368	4446	4592	4548	4548	4592	4444	4366	4288	4542	4562	4868	5172	5658
R			5524	5199	5018	4634	4534	4504	4602	4644	4752	4752	4644	4602	4501	4529	4630	5016	5197	5520	
S			6696	5660	5339	5004	4626	4688	4716	4880	4921	4920	4880	4714	4686	4624	5002	5336	5658	6696	
T				6738	5646	5292	5051	4863	4992	4978	5085	5085	4977	4992	4862	5050	5291	5644	6730		
U					7632	5808	5560	5514	5222	5217	5254	5254	5216	5222	5513	5559	5808	7627			
V						9894	7388	5856	5806	5658	5630	5630	5658	5806	5856	7384	9888				
W									9056	8286	8216	8216	8286	9050							

Fig. 16. Range of times after header uncovery for onset of channel heatup under dry steam condition

Fig. 16 shows graphically the time range for onset of channel heatup under voided conditions. This is the time at which the channel is considered fully voided and channel heatup is evaluated thereafter using the 16 ring model. This is the onset of core degradation as all previous modes of heat transfer are deemed adequate to maintain channel integrity.

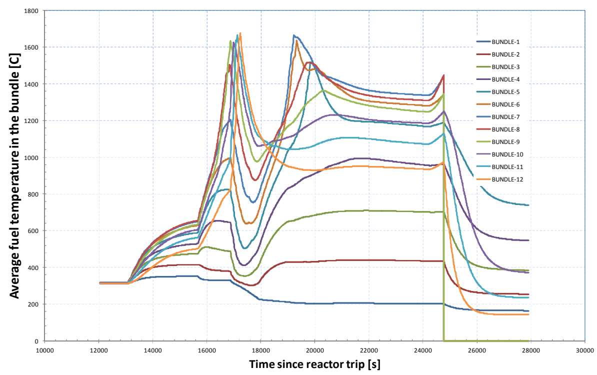

Fig. 17. Channel D-12 response in the early stages of a SBO scenario

A typical channel thermal response averaged over its 12 bundles is given in Fig. 17. There are 4 distinct periods of channel thermal response. The first period is during channel boiloff during which period the bundle temperatures are below 600°C. The early heatup is terminated by an in-core rupture in a lead channel (channel G-08 in the sample simulation) and channel cooldown during the blowdown period. The second peak indicates a termination of sheath oxidation and the third peak indicates accelerated heatup after channel uncovery. Combustible gas production over the small period of 8 hours is summarized in Fig. 18. Production of D_2 gas by steel oxidation is appreciable (~170 kg) in the first 8 hours and expected to exceed that produced by zircaloy oxidation during the first 24 hours.

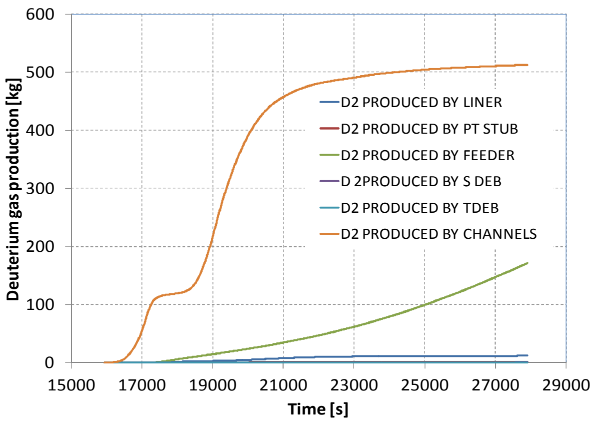

Fig. 18. H_2 production over the first 8 hours since reactor trip

These results are only for illustration purposes. A complete reanalysis of Wolsong SBO sequence is pending.

8. Summary

ISAAC is being updated to meet the current requirements and expectations. The detailed modeling of the core allows for finer estimates of the source terms. Inclusion of new severe accident phenomena is expected to allow for a greater confidence in the consequence assessments.

ACKNOWLEDGMENTS

This work was supported by the National Research Foundation of Korea (NRF) grant funded by the Korea government (Ministry of Science, ICT, and Future Planning) (No. NRF-2012M2A8A4025966).

REFERENCES

[1] KAERI(Korea Atomic Energy Research Institute), ISAAC Computer Code User's Manual, KAERI/TR-3645/2008, 2008.
[2] Modular Accident Analysis Program for CANDU Reactors, ANS 1992.
[3] IAEA TECDOC 1727 - Benchmarking Severe Accident Computer Codes for Heavy Water Reactor Applications, November 2013.
[4] NUREG/CR-7110 State-of-the-Art Reactor Consequence Analyses Project, US NRC.
[5] Recommendations and supporting Information on the Choice of Zirconium Oxidation Models in Severe accident Codes, G.Shranz, FZKA-6827, SAM-COLOSS-P043.